

Efficient Jacobian-Based Inverse Kinematics of Soft Robots by Learning

Guoxin Fang, *Student Member, IEEE*, Yingjun Tian, Zhi-Xin Yang, *Member, IEEE*,
Jo M.P. Geraedts, and Charlie C.L. Wang[†], *Senior Member, IEEE*

Abstract—This paper presents a learning-based method to solve the *inverse kinematic* (IK) problem in real-time on soft robots with highly non-linear deformation. The major challenge of efficiently computing IK for such robots is due to the lack of analytical formulation for either forward or inverse kinematics. To address this challenge, we employ neural networks to learn both the mapping function of forward kinematics and also the Jacobian of this function. As a result, Jacobian-based iteration can be applied to solve the IK problem. A sim-to-real training transfer strategy is conducted to make this approach more practical. We first generate a large number of samples in a simulation environment for learning both the kinematic and the Jacobian networks of a soft robot design. Thereafter, a sim-to-real layer of differentiable neurons is employed to map the results of simulation to the physical hardware, where this sim-to-real layer can be learned from a very limited number of training samples generated on the hardware. The effectiveness of our approach has been verified on pneumatic-driven soft robots for path following and interactive positioning.

Index Terms—Inverse Kinematics; Jacobian; Sim-to-Real; Learning; Soft Robots.

I. INTRODUCTION

WITH the use of flexible material, soft robots have the ability to make a large deformation and interact safely with the environment [1], which leads to a broad range of applications such as exoskeleton / wearable devices [2], soft manipulators [3], [4] and surgery assistance [5]. However, as a hyper-redundant system with high nonlinearity in both material propriety and geometric deformation, it is difficult to formulate an effective kinematic model for solving the control task. The analytical *forward kinematics* (FK) solution only exists for specific designs with a relatively simple shape (e.g., [6], [7]). For a general soft robot with complicated structures / shapes, computing its IK solution in real-time remains a challenging problem.

A. Related work

To efficiently model the behavior of soft robotic systems (i.e., computing FK), both analytical formulation and numer-

ical simulation were conducted in previous research. Those analytical solutions, based on differential geometry [6]–[8] and mechanics analysis [9], are difficult to be generalized for soft robots with a complex shape, where numerical simulation by the *finite element method* (FEM) is usually employed [10], [11]. Computational efficiency is a bottleneck of applying FEM in the IK computation, as the simulation needs to be repeatedly conducted to estimate the Jacobian [12]. To overcome this, a reduced model by voxel representation [13] or computing quasi-static equilibrium function of the system [14] are presented to accelerate the computation. However, these methods can easily become non-realistic after applying large rotational deformation. The geometry-oriented simulation pipeline [15] can precisely compute the deformation of a variety of soft robots even in large rotation, which is later extended into a general IK solver [16] by using the Jacobian-based iteration. A model reduction method is applied to further accelerate the numerical-based simulation [17]. However, due to the current power of computation it is still difficult to directly include the simulator in the loop of iteration and achieve real-time IK computing.

The data-driven methods used in soft robotics are often treated as regression problems of machine learning where kinematic models can be effectively learned from datasets [26]. To enable the inverse kinematic tasks on soft robots, an intuitive solution is to directly learn the mapping of IK which takes the motion as the input of a network and generates the corresponding parameters of actuation as output (ref. [18]–[24]). However, this intuitive method does not perform well in a redundant system as the one-to-many mapping from task space to actuator space is generally difficult to learn. Although this issue can be partly solved by setting constraints in the actuator space [23] or specifying the preference of configurations in the IK equation [24], we solve the problem by using a different method to combine learning with Jacobian-based IK. Our method is efficient when planning a smooth motion (i.e., by minimizing variation in the actuator space) for soft robot systems with redundancy. To reach a similar goal, Thuruthel *et al.* [27], [28] attempt to learn the differential IK model with local mapping. Another method is presented in [29] to estimate the soft robot's Jacobian by Kalman filter approximation. Recently, Bern *et al.* [25] presented a method to effectively evaluate the Jacobian by using the gradients of the FK network, which however limits the type of network used for FK learning and requires more time to compute the Jacobian for determining IK solutions. In our work, both the mapping functions of FK and the Jacobian are learned by

Manuscript prepared on December 05, 2020; revised on May 20, 2021.

G. Fang and J.M.P. Geraedts are with the Faculty of Industrial Design Engineering, Delft University of Technology, The Netherlands. G. Fang is partially supported by the China Scholarship Council for his Ph.D. study at TU Delft.

G. Fang, Y. Tian and C.C.L. Wang are with the Department of Mechanical, Aerospace and Civil Engineering, The University of Manchester, UK.

Z.-X. Yang is with the State Key Laboratory of Internet of Things for Smart City and the Department of Electromechanical Engineering, University of Macau, China.

[†]Corresponding author: changling.wang@manchester.ac.uk

TABLE I: Comparison of Training-based Methods for Solving Inverse Kinematics on Soft Robots

Property	Training Methods		
	Training for IK Mapping [18]–[24]	Jacobian by FK Network Gradient [25]	Training Jacobian & FK (Our work)
Requirement on network type	General	Analytically differentiable network	General
Smooth motion planning	Special extra effort needed [23], [24]	Yes	Yes
Target outside learning space	No	Yes	Yes
Converge speed	No iteration	Good	Good
Complexity of computation [†]	$O(hb)$	$O(hb^2)$ [‡]	$O(hb)$

[†]We evaluate the complexity of network-based IK computing on networks with $O(h)$ hidden layers and $O(b)$ neurons per layer.

[‡]The high complexity in [25] is caused by applying the chain rule to a forward kinematic network to obtain its Jacobian, which results in nested functions.

neural networks as explicit functions. This makes our method far more efficient. A comparison of three types of learning-based methods is given in Table I.

On the other hand, learning a kinematic model for soft robots usually needs a large number of samples, which can be very time-consuming when generating the data in a physical environment either by the motion capture system [4], [30] or embedded sensors [31], [32]. Moreover, to explore the boundary of the work space, a large extension in material under large actuation needs to be applied [33]. Soft materials on a robot can become fragile and might generate plastic deformation after repeating such deformation many times [4]. Consequently, the learned model becomes inaccurate. Furthermore, errors generated during the fabrication of a specimen can make the network learned on this specimen difficult to be used on other specimens with the same design.

One solution is to generate accurate dataset in the simulation environment and then convert the model learned from simulation into physical reality by transfer learning (ref. [34]–[37]). The hybrid model contains the analytical formulation and the network-based correction is conducted in [24], [38] where more precise control of the soft robot is achieved. Similarly, FEM is used in [39] to generate a simulation dataset for training a hybrid kinematic model by transfer learning, which is sufficient to use in different designs by taking advantage of numerical simulation. In this work, we study and compare the behavior of learning soft robot kinematics by using the reduced analytical model vs. the model based on numerical simulation (details are presented in Sec. IV-C). It demonstrates that many more training samples are needed to train a more complex network for fixing the reality gap [40] when the prediction generated by the reduced analytical model is less accurate than the model learned from numerical simulation. Therefore, the accurate numerical simulator [16] is used in our work to train a predictor so that only a lightweight network can be effectively trained for the sim-to-real transfer.

B. Our Method

Three networks - 1) forward kinematics \mathcal{N}_{fk} , 2) Jacobian \mathcal{N}_J , and 3) sim-to-real mapping \mathcal{N}_{s2r} are trained to support the effective computing of IK for soft robots in both virtual and physical spaces at a real-time speed. With an objective function defined in quadratic form and the network-based efficient estimation of FK and Jacobian, Jacobian-based iteration is

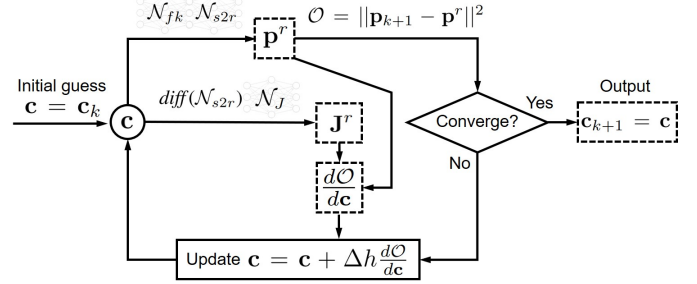


Fig. 1: Pipeline of Jacobian-based method to determine the actuation parameters \mathbf{c}_{k+1} for the way-point $\mathbf{p}_{k+1} \in \mathcal{L}$ that solves the IK problem of soft robots by minimizing $\mathcal{O}(\cdot)$ in (1). Both the position \mathbf{p}^r in task space and the Jacobian \mathbf{J}^r are effectively estimated by the networks \mathcal{N}_{fk} , \mathcal{N}_J and \mathcal{N}_{s2r} obtained from offline training. When $\mathcal{O} < \epsilon^2$, we regard the convergence as having been achieved (e.g., 0.1% of the workspace width is employed as ϵ).

used to compute the IK solution. The pipeline of our method is presented in Fig. 1 with detail discussed in Sec. II.

The technical contributions of our work are:

- A direct pipeline for learning both the FK and Jacobian from accurate numerical simulation results, to support effective IK computing for soft robots. This method can compute IK solutions in real-time and has the capability to plan a smooth motion for soft robotic systems with redundancy.
- A two-step learning strategy by using the sim-to-real transfer learning to eliminate the gap between the prediction based on simulation and the physical behavior, which can greatly reduce the required amount of empirical data when compared to directly learning a predictor from the physical experiment.

The behavior of our method has been verified on two hardware setups of soft robots giving 2D and 3D motions. The effectiveness of our method is quantitatively evaluated and compared with other approaches in the IK tasks of soft robots. Experimental tests are also conducted to demonstrate the performance of our method on soft robots with the same design but fabricated with different materials.

II. JACOBIAN-BASED KINEMATICS AND LEARNING

In this paper, we focus on solving the IK problem for soft robots – specifically, to determine the parameters of actuation that can drive a soft robot to reach a target position

/ shape. As the analytical IK solution cannot be obtained, we adopt a Jacobian-based numerical method where a target-oriented objective function $\mathcal{O}(\cdot)$ is minimized to determine the parameters of actuation. In this section, we first introduce the Jacobian-based IK computation for the path following task. After that, we demonstrate how it can be solved practically by applying the training in a virtual environment and then the sim-to-real transformation.

A. Jacobian-based IK solution

The path following problem of a soft robot is described as driving a marker on its end-effector to move along a path \mathcal{L} presented by a set of target waypoints $\{\mathbf{p}_1, \mathbf{p}_2, \dots, \mathbf{p}_i, \mathbf{p}_{i+1}, \dots\}$ in the task space. For each waypoint \mathbf{p}_i to be reached by the marker, numerical computation of inverse kinematics attempts to minimize the distance between \mathbf{p}_i and the marker's position. This is formulated as an optimization problem

$$\mathbf{c}_i = \underset{\mathbf{c}}{\operatorname{argmin}} \mathcal{O}(\mathbf{p}_i, \mathbf{c}) = \underset{\mathbf{c}}{\operatorname{argmin}} \|\mathbf{p}_i - \mathbf{p}(\mathbf{c})\|^2 \quad (1)$$

where $\mathbf{p}(\cdot) \in \mathbb{R}^n$ denotes the forward kinematic function to compute the position of the marker. The input of $\mathbf{p}(\cdot)$ is a vector of actuation parameters, $\mathbf{c} = (c_1, c_2, \dots, c_m) \in \mathbb{R}^m$. Here n and m are dimensions of the task space and the actuator space respectively.

To find the solution of (1), the gradient of $\mathcal{O}(\cdot)$ as

$$\frac{d\mathcal{O}}{d\mathbf{c}} = -2(\mathbf{p}_i - \mathbf{p}(\mathbf{c}))\mathbf{J}(\mathbf{c}) \quad (2)$$

will be employed to update the value of \mathbf{c} with $\mathbf{J}(\mathbf{c}) = d\mathbf{p}/d\mathbf{c} \in \mathbb{R}^{n \times m}$ being the Jacobian matrix that describes the moving trend of a soft robot's body at certain actuation parameters. The value of \mathbf{c} is updated by $\mathbf{c} = \mathbf{c} + \Delta h \frac{d\mathcal{O}}{d\mathbf{c}}$. Δh is a step size to minimize the value of $\mathcal{O}(\cdot)$ along the gradient direction, which can be determined by soft linear-search [16]. Fig. 1 gives the illustration of this algorithm.

When a physics-based simulation is employed to evaluate the forward kinematic function $\mathbf{p}(\cdot)$, the Jacobian matrix \mathbf{J} can be obtained by numerical difference [16], [39]. The k -th column of \mathbf{J} is computed as

$$\mathbf{J}_k = \frac{\partial \mathbf{p}(\mathbf{c})}{\partial c_k} \approx \frac{\mathbf{p}(\dots, c_k + \Delta c, \dots) - \mathbf{p}(\dots, c_k - \Delta c, \dots)}{2\Delta c}, \quad (3)$$

where Δc is a small constant determined according to experiments and assigned as $1/10N$ of the actuation range. Here N is the number of samples for each actuation parameter presented in Sec. III-B. Notice that it can be time-consuming to evaluate the values of $\mathbf{p}(\cdot)$ and $\mathbf{J}(\cdot)$ by physics-based simulation in IK computing. We therefore introduce a learning-based method to learn both the FK and the Jacobian model in the offline stage, which can support a real-time IK computing during online usage. In the meantime, the difference between the simulation and the physical behavior is fixed by the sim-to-real transfer learning.

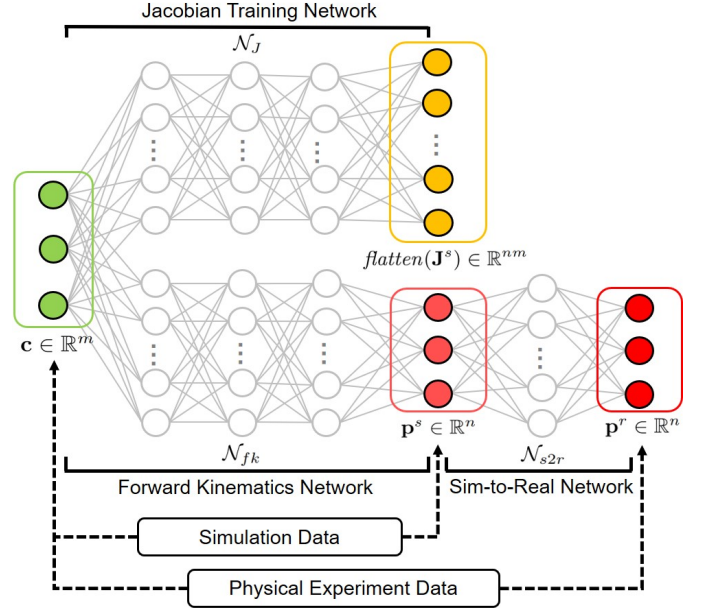


Fig. 2: The network structure used in our approach to train the kinematic model and the sim-to-real transfer.

B. Learning-based model for IK computing

We learn both the forward kinematic model and its Jacobian from simulations – denoted by $\mathbf{p}^s(\cdot)$ and $\mathbf{J}^s(\cdot)$, which are transferred to physical hardware by learning a sim-to-real mapping function $\mathbf{r}(\cdot)$. Denoting the location of a traced marker on physical hardware as \mathbf{p}^r , the function of sim-to-real mapping is required to have $\mathbf{r}(\mathbf{p}^s) \approx \mathbf{p}^r$. Neural networks are employed to learn these functions (see the architecture of neural networks shown in Fig. 2).

In the simulation environment, $\mathbf{p}^s(\cdot)$ and $\mathbf{J}^s(\cdot)$ are trained on two networks \mathcal{N}_{fk} and \mathcal{N}_J by spanning the work space of actuators with a large number of samples. Note that the output layer for \mathcal{N}_J is a column vector as the flattened Jacobian matrix \mathbf{J}^s . After obtaining the network \mathcal{N}_{fk} , the sim-to-real mapping function $\mathbf{r}(\cdot)$ is trained on a differentiable network \mathcal{N}_{s2r} by using a few samples obtained from a physical experiment conducted on the hardware setup.

With the help of these trained networks, we can estimate the Jacobian on the hardware setup as

$$\mathbf{J}^r(\mathbf{c}) = \frac{d\mathbf{p}^r}{d\mathbf{p}^s} \frac{d\mathbf{p}^s}{d\mathbf{c}} \approx \text{diff}(\mathcal{N}_{s2r})\mathbf{J}^s(\mathbf{c}) \quad (4)$$

Considering the difficulty of data acquisition on hardware specimens, the *feed-forward neuronal network* (FNN) with a single layer of fully connected neurons is adopted in our implementation for \mathcal{N}_{s2r} . The differentiation $\text{diff}(\mathcal{N}_{s2r})$ as a $n \times n$ matrix can be computed analytically by differentiating the network's activation functions. As most of the complexity in kinematics can be effectively captured by \mathcal{N}_{fk} and \mathcal{N}_J , a lightweight network \mathcal{N}_{s2r} trained by a small dataset obtained from the physical experiment can already show very good performance on eliminating the inconsistency in material properties and fabrication.

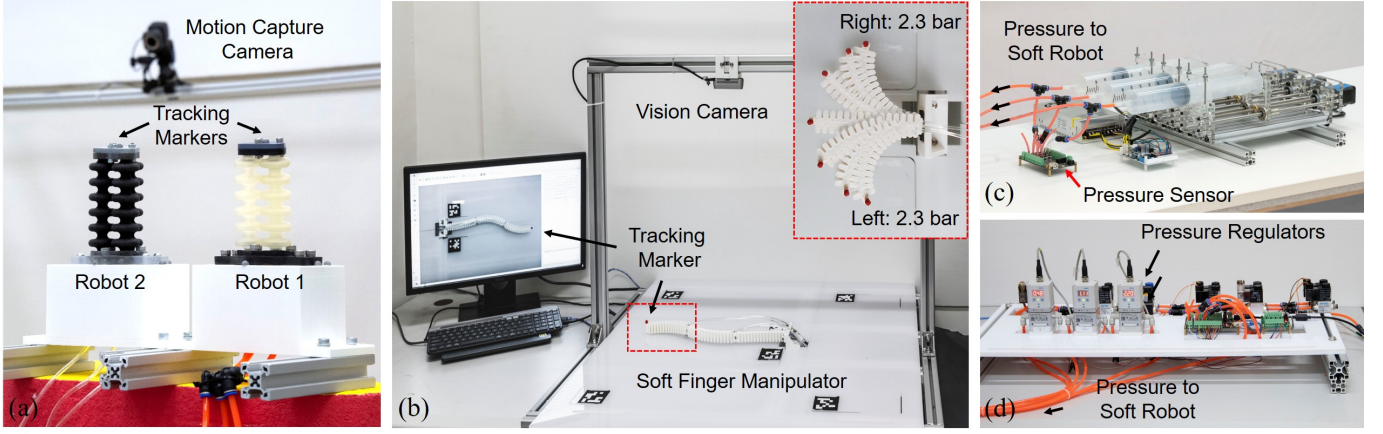


Fig. 3: Two hardware setups employed in our experiments to collect data and verify the performance of our method – (a) a soft actuator with multiple chambers that are actuated by an array of syringes (see (c)) and (b) three connected soft fingers that can be actuated individually by proportional pressure regulators (see (d)).

Through this learning-based model, the gradient of the IK objective function in the physical environment can then be computed by

$$\frac{d\mathcal{O}}{d\mathbf{c}} = -2(\mathbf{p}_i - \mathbf{p}^r(\mathbf{c}))\mathbf{J}^r(\mathbf{c}) \quad (5)$$

$$\approx -2(\mathbf{p}_i - \mathbf{r}(\mathbf{p}^s(\mathbf{c})))\text{diff}(\mathcal{N}_{s2r})\mathbf{J}^s(\mathbf{c}) \quad (6)$$

Note that the real positions of markers, $\mathbf{p}^r(\mathbf{c})$ in (5), can also be obtained from a hardware setup (e.g., by a motion-capture system). However, using positions predicted by \mathcal{N}_{fk} and \mathcal{N}_{s2r} networks can avoid physically actuating the hardware inside the loop of numerical iteration. After training the networks \mathcal{N}_{fk} , \mathcal{N}_J and \mathcal{N}_{s2r} , an iteration-based algorithm (as shown in Fig. 1) is used to effectively solve (1). The actuation parameters \mathbf{c}_{i-1} for realizing \mathbf{p}_{i-1} are employed as the initial guesses when computing \mathbf{c}_i for \mathbf{p}_i . As a result, the iteration converges rapidly and the continuity of motion in configuration space can be preserved.

III. DATA GENERATION AND TRAINING

We first present two hardware setups that are used in our research to verify the performance of the learning-based method presented above. After introducing the steps for generating datasets, the training details are provided.

A. Soft robotic hardware

Two hardware setups are constructed to investigate the performance of our IK solver. Both setups are equipped with cameras to capture the real positions of markers for the purpose of training and verification.

1) *Actuator with 3D motion*: The first setup is a 3D printed soft actuator with three chambers that can be actuated individually [4]. Its soft body can extend and bend in a 3D task space. To verify the behavior of our sim-to-real method, two specimens are fabricated by the same Object 350 Connex 3D printer but using slightly different materials – the Agilus Black and Agilus transparent materials. Both have the softness 70A according to their factory specification. These two models

are shown as Robot 1 and Robot 2 in Fig. 3(a). The soft robot is actuated by an array of syringes that has close-loop control with the help of pressure sensors as shown in Fig. 3(c). For this setup, we have the same dimension for the work space ($m = 3$) and the actuator space ($n = 3$).

2) *Planar finger manipulator*: The second setup is a soft manipulator that can move in the xy -plane (see Fig. 3(b)). The manipulator contains three soft finger sections that are rigidly connected. We use Festo Pressure Regular VPPE-3-1/8-6-010 to provide the pressure for each section (see Fig. 3(d)). Every finger section contains dual chambers that can bend symmetrically for both sides up to 120° . To maximize the deformation of each finger section, we only actuate one side for a segment each time with the pressed air in the range of $[0, 3]$ bar. When considering both sides of a segment, this results in a range of $[-3, 3]$ as actuation – i.e., ‘+’ for actuating the chamber at one side and ‘-’ for the other side. This is a redundant system with the dimension $n = 2$ for the work space and $m = 3$ in the actuator space.

B. Data generation on simulator

In our work, forward kinematics of soft robots in a virtual environment is computed by a geometry-oriented simulator [15], [16] which outperforms in its efficiency and capability to handle large rotational deformation. Therefore, this simulator is employed to generate datasets for training the forward kinematic network \mathcal{N}_{fk} and the Jacobian network \mathcal{N}_J , where the training samples of Jacobian are obtained by (3).

We now present the sampling method in actuator space for generating training data points. We uniformly divide the pressure range of each actuator into N segments to make sure that the distance between sample points is less than 1% of the workspace width. Sampling results of the two hardware setups are shown in Fig. 4, which also presents the workspaces \mathcal{P}^w of these two soft robots. In our experiment, $N = 16$ and $N = 29$ are used for these two setups respectively. This results in $16^3 = 4096$ samples for the three-chamber actuator (Fig. 4(a)) and $29^3 = 24389$ samples for the finger

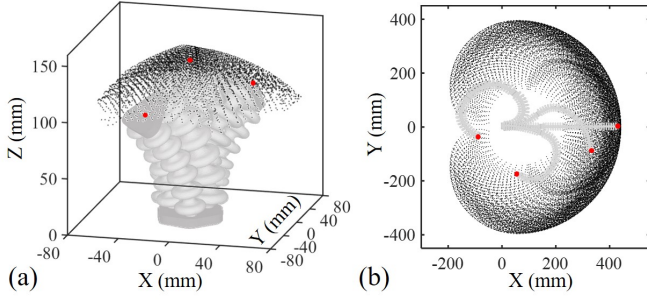


Fig. 4: The results of the simulation are employed as training samples (present in black dots) to learn the forward kinematic network \mathcal{N}_{fk} and the Jacobian network \mathcal{N}_J , where these samples also span the workspace \mathcal{P}^w of a robot. Red dots represent some example points as targets for motion in the workspace.

manipulator (Fig. 4(b)). Notice that the difference in choosing the N value is due to the redundancy of the finger setup, which also has a larger range in actuation. Based on our tests, datasets selected in these sizes can already well train \mathcal{N}_{fk} and \mathcal{N}_J to capture the kinematic behavior of soft robots (see the results in the following section). The computation time for generating each sample point is 4.3 sec. (the three-chamber robot) and 1.2 sec. (the finger manipulator) respectively.

C. Data generation on hardware

Datasets are generated by the motion capture systems mounted on the two hardware setups to train the sim-to-real network and verify the performance of our approach.

1) *Actuator with 3D motion:* To trace the 3D motion of this soft actuator, we place a marker at the center of its top plane and several markers on its static base. The motion capture system that contains 8 Vicon Bonita 10 cameras and 10 Vicon Vantage 5 cameras is used to capture the movements at the rate of 30 Hz. Because of the viscoelasticity of soft materials used to fabricate this robot, it takes a relatively long time for the position of a marker to become stable (i.e., less than 0.05mm change between neighboring image frames). This makes the process of data collection more time-consuming than a robotic system with rigid bodies. As a result, the average time for collecting one sample in the physical environment is 4.0 sec.

2) *Planar finger manipulator:* As only planar coordinates are needed when tracking the positions of a marker, we use a RealSense D435 camera mounted at the top of the setup. We place a red marker on the tip of the manipulator and adopt the OpenCV library as software to track the marker's position in the plane. QR code is employed to build the mapping between the coordinates in image space and the coordinates in the real world. The speed of data acquisition for this system is 10 Hz. For this hardware setup, the average time for collecting one sample point is 3.5 sec.

D. Details of training

In our experiment, FNN is employed for all three networks as FNN can adequately capture the nonlinear behavior in a training dataset, including the many-to-one forward kinematic

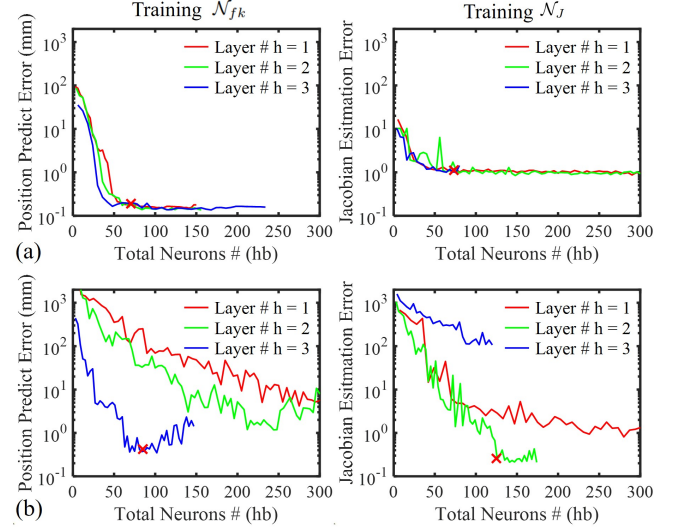


Fig. 5: Comparison of learning results by using a different number of layers as h and a different number of neurons b per layer (i.e., the total number of neurons in a network is hb). Tests are conducted on (a) the robotic setup without redundancy (the three-chamber actuator with $m = n = 3$) vs. (b) the setup with redundancy (the planar finger manipulator having $m = 3$ and $n = 2$). Red crosses indicate the network parameters used in the physical experiment.

mapping for redundant systems. All networks are trained by using the Deep Learning Toolbox of Matlab running on an NVIDIA GeForce RTX 2070 graphics card. We first study the effectiveness of training \mathcal{N}_{fk} and \mathcal{N}_J by using a different number of layers and different numbers of neurons. Each data set is divided into training, validation, and test subsets in the ratio of 70% : 20% : 10%. The Tan-Sigmoid is set as the activation function for FNN. The maximum number of epochs $MaxN_{Epoc} = 13500$ and the learning rate $\tau = 0.04$ are employed. The tests are conducted on both hardware setups. The estimation errors are evaluated on the test datasets as shown in Fig. 5.

It is found that the structure of the network for learning the Jacobian \mathcal{N}_J on a redundant system (i.e., the planar finger manipulator) needs to be selected more carefully. The best performance is observed on this hardware setup when FNN with $h = 2$ hidden layers and $b = 64$ neurons per layer is employed to learn \mathcal{N}_J . Differently, FNN with $h = 3$ layers and $b = 30$ neurons per layer gives the best results in training \mathcal{N}_{fk} . The error of position prediction by using \mathcal{N}_{fk} is less than 0.5 mm (i.e., 0.58% of the work space's width). For the three-chamber actuator, the numbers of layers and neurons have less influence on the training result. For this setup, we select $h = 2$ and $b = 35$ for both networks, which results in a FK prediction with error less than 0.17 mm on the test dataset (i.e., 0.34% of the workspace's width). With such accurate predictions generated by \mathcal{N}_{fk} and \mathcal{N}_J , we can obtain IK solutions efficiently and accurately (see the behavior study given in Section IV).

When training for \mathcal{N}_{s2r} , we have to select a network that has differentiation in analytic form and also has a smaller number of neurons, as the network has to be trained from physical

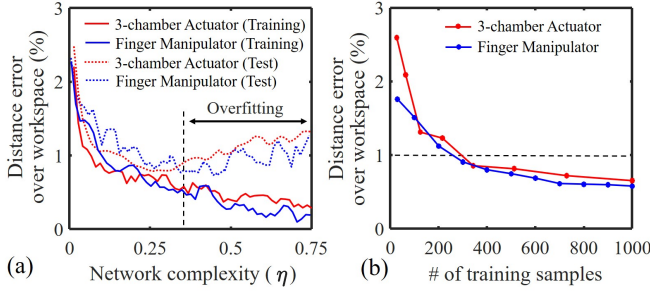


Fig. 6: Experimental study for the performance influence in the sim-to-real network \mathcal{N}_{s2r} by using (a) different numbers of neurons and (b) datasets in different sizes. With the properly selected complexity of network structure, the over-fitting problem can be avoided. The distance predict error can be controlled within 1% of the workspace width for both setups when a limited number of training samples are used (see (b)).

experiments. Therefore, we employ a single layer of fully connected neurons using Tan-Sigmoid as the activation function. An important parameter here is the number of neurons, which is selected as η times the number of samples to avoid over-fitting on the test dataset. For each hardware setup, we generate a benchmark dataset with around 1,000 randomly selected samples that span the whole space of actuation. Respectively, 700 and 300 sample points are used for the training and the test datasets. Fig. 6(a) presents the behavior on both the training dataset (denoted by the solid curves) and the test dataset (denoted by the dash curves) when using different values of η . Based on the analysis, $\eta = 1/4$ is selected for our experiment to avoid over-fitting.

As the time used to collect physical data points should be controlled, we also study the behavior of \mathcal{N}_{s2r} with different numbers of training samples. For this purpose, the prediction errors as the ratios of the distance errors over the workspace widths are given in Fig. 6(b) to study the effectiveness of using different numbers of samples. In these tests, the number of neurons is always assigned as $\eta = 1/4$ of the training samples. For both setups, we find that the network \mathcal{N}_{s2r} can be well trained when using a limited number of training samples. In our implementation, 1% is selected as the threshold of accurate prediction and this threshold is used to determine the number of samples for training \mathcal{N}_{s2r} . As a result, 343 samples are used for the three-chamber actuator and 620 samples are conducted for the finger manipulator. The datasets for training \mathcal{N}_{s2r} on the two hardware setups can both be collected within 30 min in our physical experiment.

IV. EXPERIMENT RESULTS AND DISCUSSION

In this section, we present all the experiment results of IK computing for soft robots by using our learning based Jacobian iteration. The results are generated in both the virtual and the physical environments. Computation of the learned neural networks in prediction is implemented in C++ and integrated into our control platform to gain the best computational efficiency. All the IK computations can run in real-time on a laptop PC with Intel i7-9750H 2.60GHz CPU and 16GB

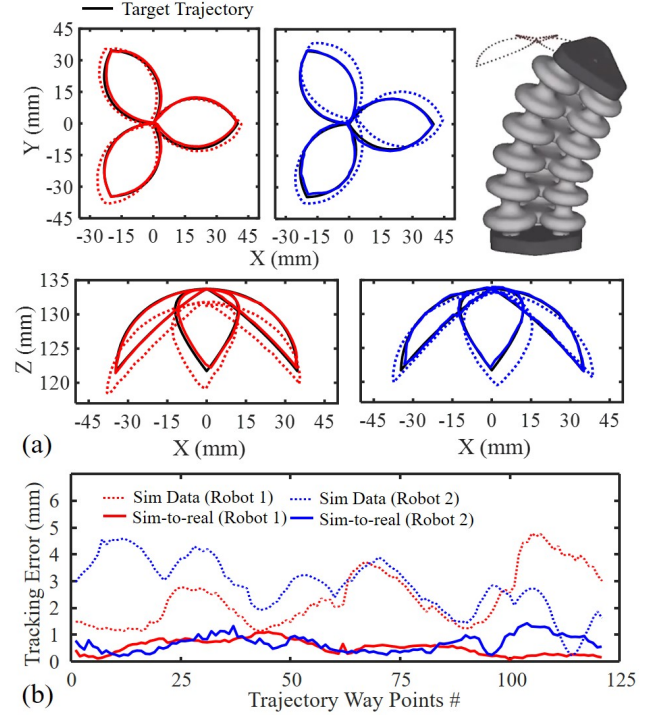


Fig. 7: Results of path following task on two soft robots – i.e., Robot 1 (R1) and Robot 2 (R2) with the same design but fabricated with different materials (see also Fig. 3(a)). Both the trajectories before and after applying the sim-to-real network are captured by the motion capture system and displayed in (a). Compared to the target trajectory (shown as black curves in (a)), the distance errors at all waypoints are shown in (b). After applying the sim-to-real network, the maximal errors for both robots are less than 1.2 mm.

memory. Note that the prediction made by networks and the IK algorithm is entirely run on a CPU.

A. Path following

1) *Actuator with 3D motion:* We test the behavior of path following for a desired 3D trajectory contains 125 waypoints. When running in the simulation environment, the trained networks can generate actuation parameters resulting in very accurate trajectories. The average tracking error is 0.13 mm. In short, the result of Jacobian-based IK computation by learning has a similar accuracy to the simulation-based method [16] with an average error of 0.13 mm, but with a substantial improvement in efficiency.

In the physical environment, we learn the sim-to-real networks separately on two soft robots as shown in Fig. 3(a). If we directly apply the actuation parameters obtained from IK computing in a simulation environment, the error of path following is high (i.e., up to 5 mm). At the same time, the variation caused by fabrication and material can be clearly observed from the difference between R1 and R2, as shown in Fig. 7. By incorporating the sim-to-real transfer in our method, we can successfully reduce the error in the physical environment to less than 1.2 mm for both robots (see Fig. 7(b)), which is 1.71% of the workspace width.

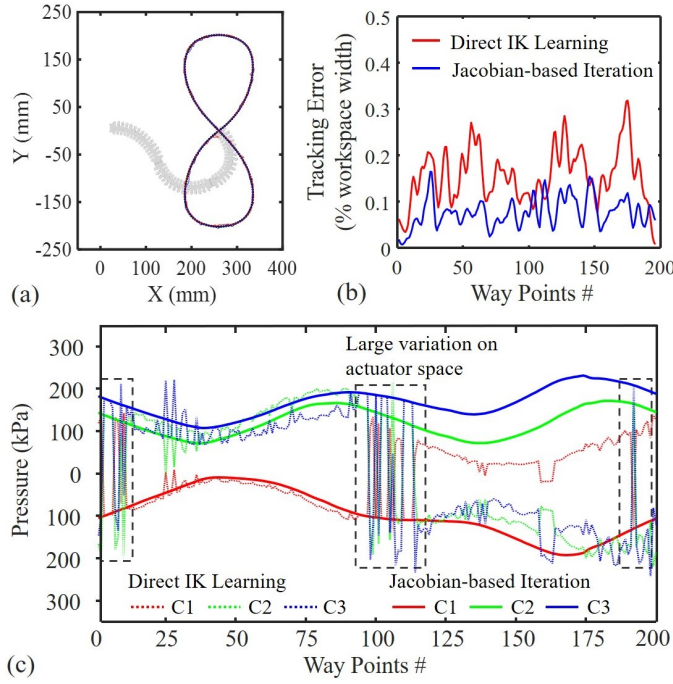


Fig. 8: For realizing the ‘8’-shape trajectory shown in (a) by the soft finger manipulator, the actuation parameters (pressure) in each soft finger segment are computed to realize the trajectory. (b) Comparison of tracking errors in the task space from the direct IK learning vs. the Jacobian-based iteration by learning (our method). (c) Visualization of IK solutions in the actuator space, where C1, C2 & C3 present the actuation parameters (i.e., pressures) in three different chambers – large variation can be found from the results obtained by direct IK learning.

2) *Planar finger manipulator*: This is a redundant system, in other words, 3-DOFs actuation with 2-DOFs in motion. Therefore, an input waypoint can have multiple solutions in the actuator parameters. To avoid the large variation in the sequence of actuation for neighboring waypoints, we apply the planning algorithm presented in [16], which takes the actuation parameters determined for the previous waypoint as the initial guess for the IK computation. This strategy can help the computation converge in a few iterations and avoid large variations in configurations.

The results of following an ‘8’-shape trajectory that contains 200 way points are shown in Fig. 8(a). The actuation parameters obtained from the Jacobian-based method are compared with those resulting from direct IK-learning. For both results in the xy -plane, the tracking errors are less than 1.2 mm in the virtual environment, in other words, 0.3% of the workspace width. Moreover, our Jacobian-based IK by learning demonstrates excellent performance in the accuracy of tracking precision. The average and maximum tracking errors for all waypoints are 0.08% and 0.18% of the workspace width, respectively. Large variation (i.e., jumps) in the actuator space can be found in the results of direct IK-learning as shown in Fig. 8(c). This problem of direct IK learning is mainly caused by its lack of capability to support the one-to-many IK mapping. Significantly improved smoothness in motion can be observed in the results generated by our Jacobian-based

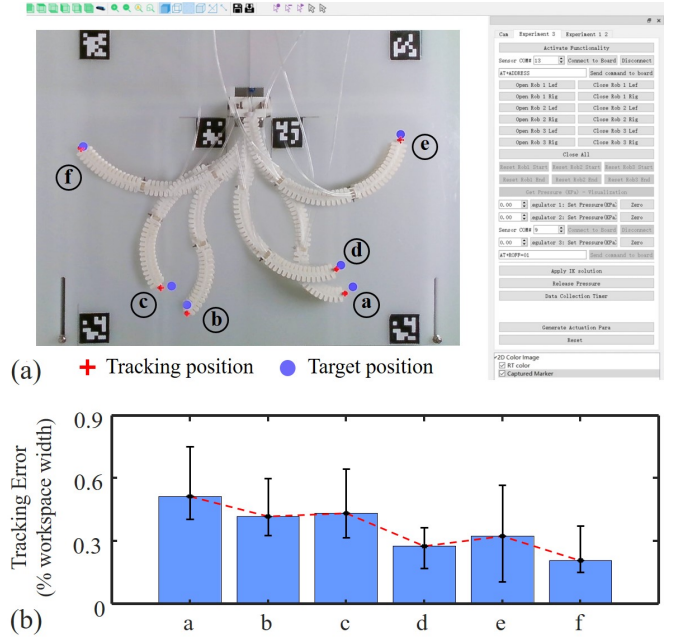


Fig. 9: Interactive positioning results for the soft manipulator with three finger actuators. (a) With a user-specified position given through the software interface, our Jacobian-based method is applied to determine the IK solution. (b) The bar chart presents the tracking errors for different target positions, where the repeatability is also studied and displayed as the range of deviation in tracking errors.

method (see also the supplementary video). The IK solutions can be efficiently computed by our method at the average speed of 39 ms per waypoint.

B. Interactive positioning

The experiment of interactive positioning is also conducted on the soft manipulator with three finger segments. By using the hardware setup with a camera, we have realized an interactive positioning function on the soft manipulator. As shown in Fig. 9(a), users can select the desired point location for the manipulator’s tip through our interface and our planner will compute the IK solutions as the corresponding actuation parameters. The computation can be completed in real-time. As a result, users can interactively position the manipulator’s tip – see also the supplementary video. When different positions are selected in the work space, the soft manipulator can move among configurations with large variations.

The errors of positioning are evaluated with the help of camera as the distances between the user-specified position and the physically realized position on the soft manipulator. The errors are given in Fig. 9(b) as a bar chart. It is found that all six target positions can be realized in the physical environment with tracking errors less than 0.9% of the work space’s width. Note that, each of these six target positions is tested 10 times in random order to study the repeatability of our system. The results are displayed as the range of derivation on the bar chart.

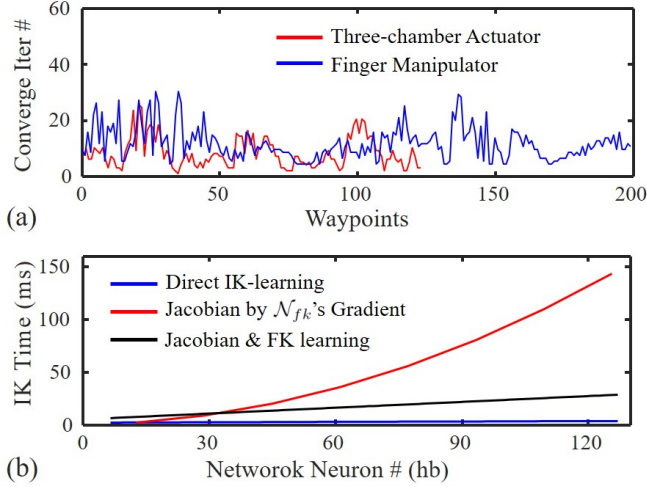


Fig. 10: Quantitative analysis for (a) the speed of convergence and (b) the time efficiency of our Jacobian-based training method. Three learning strategies for computing IK are compared in (b).

C. Discussion

1) *Analysis of computing speed:* An advantage of our approach is its computation efficiency. Compared with the simulation-in-the-loop method [16], our learning-based method can reach more than $750\times$ speedup when solving IK problems for soft robots. Although our method is based on iterations, it converges rapidly. As illustrated in Fig. 10(a), our method can converge in an average 8.2 and 9.3 iterations for the IK tasks of the three-chamber actuator and the finger manipulator, respectively. The termination condition of iteration as given in Fig. 1 is used in these tests.

We also test the IK computing speeds by setting a fixed number of iteration steps as 10 and comparing the efficiency among three different learning-based methods. As shown in Fig. 10(b), when the same number of neurons is employed, the direct IK learning method is the most efficient as no iteration is needed. As discussed in Table I, our method shows a linear complexity that ensures a real-time speed (i.e. 28 ms per waypoint when the maximal number of neurons $hb = 128$ is used in physical experiments). It supports the IK computation at the rate of 35+ waypoints per second. In contrast, for the method that only learns \mathcal{N}_{fk} and evaluates Jacobian by computing the gradient of \mathcal{N}_{fk} (ref. [25]), 138 ms per waypoint is required for IK computation on average (with $hb = 128$). This can only reach the rate of 7.25 waypoints per second.

2) *Initial-value, singularity, and redundancy:* When realizing the path following tasks on redundant systems, our method can outperform the direct IK learning solution as already discussed in Sec. IV-A. Thus, minimal variation in actuator space is naturally guaranteed. In our method, the configuration of motion is highly dependent on the selection of the IK solution at the starting waypoint (i.e., the initial value). As demonstrated in Fig. 11, the configuration of the finger manipulator determined by our IK solver at a waypoint is always close to the IK solution of the previous waypoint

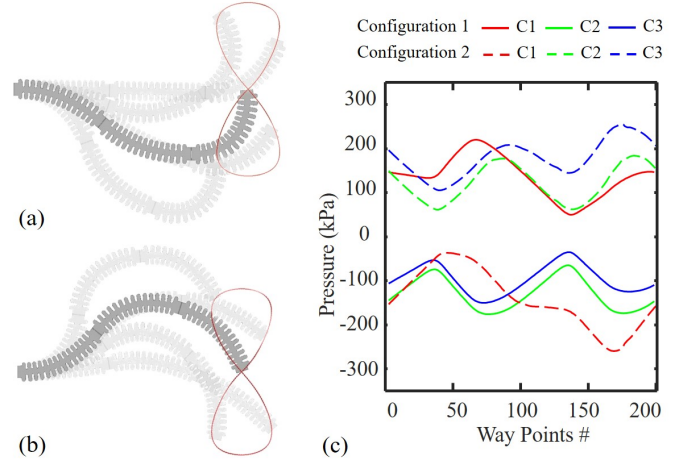


Fig. 11: Two different configurations of motion are shown in (a) and (b), both of which are feasible IK solutions for following the '8'-shape path by the soft finger manipulator. The smoothness in motion is guaranteed by the Jacobian-based iteration for both results as shown in (c), where the actuation in every chamber has minimal variation in control parameters between neighboring waypoints.

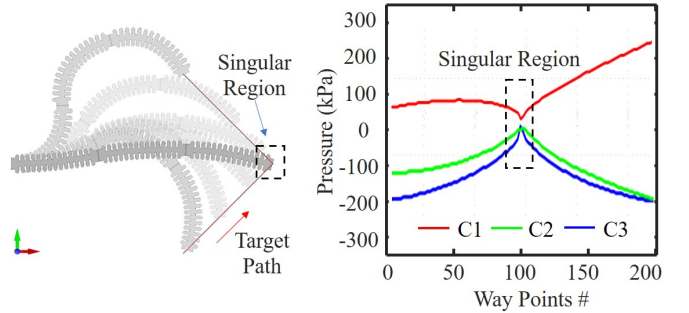


Fig. 12: Results for the path following task passing through the singularity region. Our method can successfully compute feasible smooth motions when meeting singularity.

where this dependency can trace back to the beginning point. This is because our Jacobian-based iteration tends to minimize the distance-based objective function defined in (1) while minimizing the change in actuation parameters. This preferred property is also kept when computing IK solutions for a motion passing through the singularity region (see the example in Fig. 12). As a Jacobian-based iterative solver, our method can always generate a nearly optimal solution for singularity points by applying appropriate terminal conditions (e.g., minimal variation in the value of the objective function).

On the other hand, it is worth noting that the proposed method cannot yet fully control the redundancy in IK computing (i.e., choosing the configuration based on user preference). For the interactive positioning experiment shown in Sec. IV-B, our method can generate results in different configurations for two close waypoints (e.g., the point b and c shown in Fig. 9) when using initial values that are always far from the resultant configurations (zero is adopted for all actuation parameters in this case). However, when using the IK solution of b as initial values to compute the IK solution for c, the resultant configuration of point c will be similar to the configuration

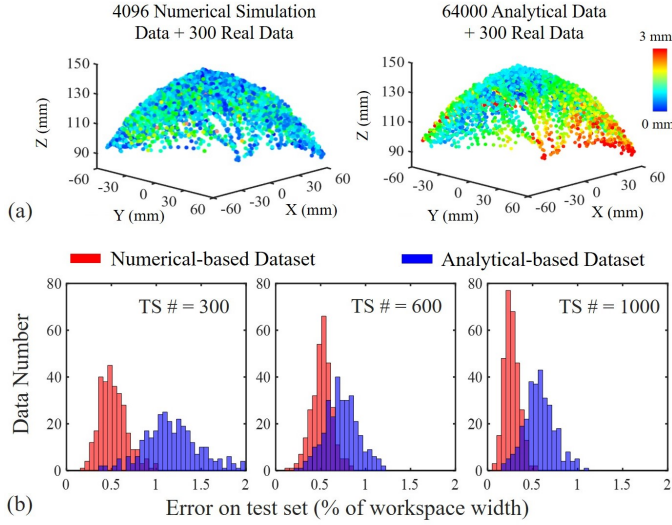


Fig. 13: Comparison for studying the performance of sim-to-real learning on 1) numerical simulation-based (our approach) vs. 2) analytical computation-based (ref. [4], [8]) training datasets. The experiments are conducted on the three-chamber soft actuator setup (i.e., the hardware shown in Fig. 3(a)). (a) Visualization of prediction errors in the task space. The colors of points represent the errors in the distance. (b) Histograms show the distributions of prediction errors when using different numbers (mark as TS #) of samples to train \mathcal{N}_{s2r} . Note that the number of neurons for the sim-to-real network \mathcal{N}_{s2r} is chosen as $1/4$ of TS #.

of b. In short, our method works well to determine one IK solution instead of all feasible IK solutions, and which IK solution is generated by our solution relies heavily on the initial value feeding to the Jacobian-based iteration. In our future work to better control the redundancy of soft robotic systems, we plan to investigate the clustering strategy applied in the task space [41] and the feasibility of adding regularization terms into the objective function [24].

3) *Numerical simulation vs. analytical model*: In our implementation, an accurate numerical simulator is employed to generate datasets for training \mathcal{N}_{fk} and \mathcal{N}_J . The purpose is to reduce the gap between the results estimated by \mathcal{N}_{fk} and the physical results. Differently, when the dataset for training is obtained from an analytical model, the gap becomes larger. As a result, more empirical samples are needed for training the sim-to-real network \mathcal{N}_{s2r} to achieve the same level of accuracy. The comparison in terms of prediction accuracy by using different strategies is presented in Fig. 13, where the analytical model based on differential geometry (ref. [4], [8]) is used to compare with our method. As observed in Fig. 13(a), the model trained by the dataset obtained from the numerical simulation (i.e., our approach) shows smaller prediction errors when using the same number of samples to learn the sim-to-real network \mathcal{N}_{s2r} . Note that this less accurate result is still observed even after using more samples generated from the analytical model (e.g., 64000 in our experiment) when the number of real samples is fixed.

This experiment also proves that the sim-to-real network can effectively eliminate the gap between simulation and reality – although requiring different numbers of samples for the model

learned from numerical simulation (i.e., our method) and the analytical model. As an example, Fig. 13(b) shows that the accuracy within 1% of the workspace width can be obtained at most points when TS# = 300 and TS# = 1000 are used by our method and the analytical model respectively. As a general case, it is more costly to generate a large number of physical training samples than simulation-based samples. Generating a dataset of empirical samples in a large number is very time-consuming and may result in material failure. Our method proposed in this paper converts this challenge into an approach that is easier to realize, in other words, learning a more accurate predictor from more accurate samples generated by numerical simulation. As a result, the gap between prediction and reality can be reduced and fixed by a light sim-to-real network.

4) *Limitation*: One major drawback of our learning-based method is the time needed for generating datasets in a virtual environment, as more samples are needed than for only training the FK network. For a Jacobian sample point, the simulation needs to run $2m$ times for computing the $n \times m$ matrix \mathbf{J}^s by numerical differences. However, this complexity is still linear and can be easily executed in parallel on the multi-core CPU of a computer. Moreover, we plan to use the method presented in [42] to evaluate the Jacobian more efficiently in our future work.

V. CONCLUSION

In this paper, we present a method to train the forward kinematic model and its Jacobian together as two neural networks to realize the real-time computation of inverse kinematics on soft robots, which is formulated as an optimization problem. As our method can generate smooth motion in a redundant system, it outperforms the existing approaches of direct IK learning. Considering the difficulty in generating large datasets on hardware setups, we adopt a highly effective simulator to generate the training datasets and later apply a sim-to-real network to transfer the kinematic model onto hardware. A lightweight network is employed for sim-to-real mapping so that it can be trained by using a small number of samples. This sim-to-real strategy allows our approach to work on different soft robots that have variations caused by materials and fabrication processes. The main advantages of our method include the efficient computation and the ease of applying the sim-to-real learning transfer.

We test the behavior of our learning-based method in the tasks of path following and interactive positioning on two different soft robotic setups. Our method can solve the IK problem for soft robots in real-time and make a good control for the kinematic tasks. As a future work, we plan to explore the possibility of using time-related data for sim-to-real transfer learning that may further enhance the accuracy of IK computing. Moreover, integrating our method of kinematic computation into controllers while considering interaction and obstacle avoidance will also be investigated in the future.

REFERENCES

- [1] D. Rus and M. Tolley, “Design, fabrication and control of soft robots,” *Nature*, vol. 521, pp. 467–75, 05 2015.

- [2] P. Polygerinos, Z. Wang, K. C. Galloway, R. J. Wood, and C. J. Walsh, "Soft robotic glove for combined assistance and at-home rehabilitation," *Robotics and Autonomous Systems*, vol. 73, pp. 135–143, 2015.
- [3] A. Melingui, O. Lakhal, B. Daachi, J. B. Mbode, and R. Merzouki, "Adaptive neural network control of a compact bionic handling arm," *IEEE/ASME Transactions on Mechatronics*, vol. 20, no. 6, pp. 2862–2875, 2015.
- [4] D. Drotman, M. Ishida, S. Jadhav, and M. T. Tolley, "Application-driven design of soft, 3d printed, pneumatic actuators with bellows," *IEEE/ASME Transactions on Mechatronics*, 2018.
- [5] T. Ranzani, G. Gerboni, M. Cianchetti, and A. Menciassi, "A bioinspired soft manipulator for minimally invasive surgery," *Bioinspiration & Biomimetics*, vol. 10, no. 3, p. 035008, may 2015.
- [6] G. S. Chirikjian and J. W. Burdick, "A modal approach to hyper-redundant manipulator kinematics," *IEEE Transactions on Robotics and Automation*, vol. 10, no. 3, pp. 343–354, Jun. 1994.
- [7] B. A. Jones and I. D. Walker, "Kinematics for multisection continuum robots," *IEEE Transactions on Robotics*, vol. 22, no. 1, pp. 43–55, Feb. 2006.
- [8] M. Rolf and J. J. Steil, "Constant curvature continuum kinematics as fast approximate model for the bionic handling assistant," in *IEEE/RSJ International Conference on Intelligent Robots and Systems*, 2012, pp. 3440–3446.
- [9] F. Renda, M. Giorelli, M. Calisti, M. Cianchetti, and C. Laschi, "Dynamic model of a multibending soft robot arm driven by cables," *IEEE Transactions on Robotics*, vol. 30, no. 5, pp. 1109–1122, Oct. 2014.
- [10] P. Moseley, J. M. Florez, H. A. Sonar, G. Agarwal, W. Curtin, and J. Paik, "Modeling, design, and development of soft pneumatic actuators with finite element method," *Advanced engineering materials*, vol. 18, no. 6, pp. 978–988, 2016.
- [11] M. S. Xavier, A. J. Fleming, and Y. K. Yong, "Finite element modeling of soft fluidic actuators: Overview and recent developments," *Advanced Intelligent Systems*, vol. 3, no. 2, p. 2000187, 2021.
- [12] D. E. Orin and W. W. Schrader, "Efficient computation of the jacobian for robot manipulators," *The International Journal of Robotics Research*, vol. 3, no. 4, pp. 66–75, 1984.
- [13] J. Hiller and H. Lipson, "Dynamic simulation of soft multimaterial 3d-printed objects," *Soft Robotics*, vol. 1, no. 1, pp. 88–101, 2014.
- [14] C. Duriez, "Control of elastic soft robots based on real-time finite element method," in *2013 IEEE International Conference on Robotics and Automation*, May 2013, pp. 3982–3987.
- [15] G. Fang, C. Matte, T. Kwok, and C. C. L. Wang, "Geometry-based direct simulation for multi-material soft robots," in *2018 IEEE International Conference on Robotics and Automation (ICRA)*, 2018, pp. 4194–4199.
- [16] G. Fang, C. D. Matte, R. B. N. Scharff, T. H. Kwok, and C. C. L. Wang, "Kinematics of soft robots by geometric computing," *IEEE Transactions on Robotics*, vol. 36, no. 4, pp. 1272–1286, 2020.
- [17] O. Gouy and C. Duriez, "Fast, generic, and reliable control and simulation of soft robots using model order reduction," *IEEE Transactions on Robotics*, vol. 34, no. 6, pp. 1565–1576, 2018.
- [18] M. Giorelli, F. Renda, G. Ferri, and C. Laschi, "A feed-forward neural network learning the inverse kinetics of a soft cable-driven manipulator moving in three-dimensional space," in *2013 IEEE/RSJ International Conference on Intelligent Robots and Systems*, 2013, pp. 5033–5039.
- [19] M. Giorelli, F. Renda, G. Ferri, and C. Laschi, "A feed forward neural network for solving the inverse kinetics of non-constant curvature soft manipulators driven by cables," in *Dynamic Systems and Control Conference*, vol. 56147. American Society of Mechanical Engineers, 2013, p. V003T38A001.
- [20] M. Rolf and J. J. Steil, "Efficient exploratory learning of inverse kinematics on a bionic elephant trunk," *IEEE Transactions on Neural Networks and Learning Systems*, vol. 25, no. 6, pp. 1147–1160, 2014.
- [21] M. Giorelli, F. Renda, M. Calisti, A. Arienti, G. Ferri, and C. Laschi, "Neural network and jacobian method for solving the inverse statics of a cable-driven soft arm with nonconstant curvature," *IEEE Transactions on Robotics*, vol. 31, no. 4, pp. 823–834, 2015.
- [22] J. Chen and H. Y. K. Lau, "Learning the inverse kinematics of tendon-driven soft manipulators with k-nearest neighbors regression and gaussian mixture regression," in *2016 2nd International Conference on Control, Automation and Robotics (ICCAR)*, 2016, pp. 103–107.
- [23] R. Grassmann, V. Modes, and J. Burgner-Kahrs, "Learning the forward and inverse kinematics of a 6-dof concentric tube continuum robot in se(3)," in *IEEE/RSJ International Conference on Intelligent Robots and Systems*, 2018, pp. 5125–5132.
- [24] R. F. Reinhart, Z. Shareef, and J. J. Steil, "Hybrid analytical and data-driven modeling for feed-forward robot control," *Sensors*, vol. 17, no. 2, p. 311, 2017.
- [25] J. M. Bern, Y. Schnider, P. Banzet, N. Kumar, and S. Coros, "Soft robot control with a learned differentiable model," in *2020 IEEE International Conference on Soft Robotics (RoboSoft)*, 2020, pp. 417–423.
- [26] T. George Thuruthel, Y. Ansari, E. Falotico, and C. Laschi, "Control strategies for soft robotic manipulators: A survey," *Soft Robotics*, vol. 5, no. 2, pp. 149–163, 2018, pMID: 29297756.
- [27] T. G. Thuruthel, E. Falotico, M. Cianchetti, F. Renda, and C. Laschi, "Learning global inverse statics solution for a redundant soft robot," in *Proceedings of the 13th International Conference on Informatics in Control, Automation and Robotics - Volume 2: ICINCO*, INSTICC. SciTePress, 2016, pp. 303–310.
- [28] T. G. Thuruthel, E. Falotico, M. Cianchetti, and C. Laschi, "Learning global inverse kinematics solutions for a continuum robot," in *Symposium on Robot Design, Dynamics and Control*. Springer, 2016, pp. 47–54.
- [29] M. Li, R. Kang, D. T. Branson, and J. S. Dai, "Model-free control for continuum robots based on an adaptive kalman filter," *IEEE/ASME Transactions on Mechatronics*, vol. 23, no. 1, pp. 286–297, 2018.
- [30] T. G. Thuruthel, E. Falotico, F. Renda, and C. Laschi, "Model-based reinforcement learning for closed-loop dynamic control of soft robotic manipulators," *IEEE Transactions on Robotics*, vol. 35, no. 1, pp. 124–134, 2019.
- [31] T. G. Thuruthel, B. Shih, C. Laschi, and M. T. Tolley, "Soft robot perception using embedded soft sensors and recurrent neural networks," *Science Robotics*, vol. 4, no. 26, 2019.
- [32] R. B. N. Scharff, R. M. Doornbusch, E. L. Doubrovski, J. Wu, J. M. P. Geraedts, and C. C. L. Wang, "Color-based proprioception of soft actuators interacting with objects," *IEEE/ASME Transactions on Mechatronics*, vol. 24, no. 5, pp. 1964–1973, 2019.
- [33] Y. Sun, Y. S. Song, and J. Paik, "Characterization of silicone rubber based soft pneumatic actuators," in *2013 IEEE/RSJ International Conference on Intelligent Robots and Systems*, 2013, pp. 4446–4453.
- [34] E. S. Marquez, J. S. Hare, and M. Niranjan, "Deep cascade learning," *IEEE Transactions on Neural Networks and Learning Systems*, vol. 29, no. 11, 2018.
- [35] S. Kriegman, A. M. Nasab, D. Shah, H. Steele, G. Branin, M. Levin, J. Bongard, and R. Kramer-Bottiglio, "Scalable sim-to-real transfer of soft robot designs," in *IEEE International Conference on Soft Robotics*, 2020, pp. 359–366.
- [36] H. Park, J. Cho, J. Park, Y. Na, and J. Kim, "Sim-to-real transfer learning approach for tracking multi-dof ankle motions using soft strain sensors," *IEEE Robotics and Automation Letters*, vol. 5, no. 2, pp. 3525–3532, 2020.
- [37] H. Donat, S. Lilge, J. Burgner-Kahrs, and J. J. Steil, "Estimating tip contact forces for concentric tube continuum robots based on backbone deflection," *IEEE Trans. Med. Robot. Bionics*, vol. 2, no. 4, 2020.
- [38] M. S. Malekzadeh, S. Calinon, D. Bruno, and D. G. Caldwell, "Learning by imitation with the stiff-flop surgical robot: a biomimetic approach inspired by octopus movements," *Robotics and Biomimetics*, vol. 1, no. 1, pp. 1–15, 2014.
- [39] M. Wiese, G. Runge, B.-H. Cao, and A. Raatz, "Transfer learning for accurate modeling and control of soft actuators," in *2021 IEEE International Conference on Soft Robotics (RoboSoft)*, 2021.
- [40] S. Koos, J. Mouret, and S. Doncieux, "The transferability approach: Crossing the reality gap in evolutionary robotics," *IEEE Transactions on Evolutionary Computation*, vol. 17, no. 1, pp. 122–145, 2013.
- [41] A. Jiohou Kouabon, A. Melingui, J. Mvogo Ahanda, O. Lakhal, V. Coelen, M. KOM, and R. Merzouki, "A learning framework to inverse kinematics of high dof redundant manipulators," *Mechanism and Machine Theory*, vol. 153, p. 103978, 2020.
- [42] D. Navarro-Alarcón, Y. H. Liu, J. G. Romero, and P. Li, "Model-free visually servoed deformation control of elastic objects by robot manipulators," *IEEE Transactions on Robotics*, vol. 29, no. 6, pp. 1457–1468, 2013.